

# Formation mechanism and suitable controlling pattern of sand hazards at Honglianghe River section of Qinghai–Tibet Railway

Shengbo Xie · Jianjun Qu · Yuanming Lai · Yingjun Pang

Received: 19 July 2014 / Accepted: 6 November 2014 / Published online: 12 November 2014  
© Springer Science+Business Media Dordrecht 2014

**Abstract** The sand hazards at Honglianghe River section of Qinghai–Tibet Railway are serious, and the effect of controlling measures is limited because the disaster-causing mechanism is currently unclear. The source of sandy materials, blown sand power environment, and controlling measures of Honglianghe River section were investigated by using methods such as field observation and analysis and indoor calculation to understand the sand hazard rules of Qinghai–Tibet Railway systematically. The sandy materials discovered are mainly from the sandy hill of the west side of the railway. In addition, the grain composition of sand with particle size in the range of 0.25–0.10 mm is given priority. Yearly sand-moving winds are usually from the N, NNW, and NW directions. The frequencies of these three wind groups accounted for 85.16 % of the yearly total. The most serious sand hazards were located at the NW direction of the railway. The yearly sand drift potential (DP) is 270.57 vector units (VU), the yearly resultant drift potential (RDP) is 247.27 VU, the yearly direction variability index (RDP/DP) is 0.91, and the yearly resultant drift direction is 162.84°. In windy dry season (during the colder half of the year), loose and broken sand materials are blown up by wind, forming wind–sand flow and movement, which are then blocked by the railway subgrade, and accumulate and thus cause disaster. We propose that the sand-controlling pattern of Qinghai–Tibet Railway is dominated by sand blocking and sand fixing, namely sand blocking in the outer fringe and sand fixing in the inner fringe, supplemented by sand transport and sand diversion, combined with vegetation. This pattern can be a significant reference to controlling sand hazards in other similar zones.

---

S. Xie (✉) · J. Qu · Y. Lai  
Key Laboratory of Desert and Desertification/State Key Laboratory of Frozen Soil Engineering/  
Dunhuang Gobi and Desert Research Station, Cold and Arid Regions Environmental and Engineering  
Research Institute, Chinese Academy of Sciences, Lanzhou 730000, China  
e-mail: xiashengbo@lzb.ac.cn

Y. Pang  
Institute of Desertification Studies, Chinese Academy of Forestry, Beijing 100091, China

**Keywords** Qinghai–Tibet Railway · Sand-moving wind · Drift potential · Sand hazards · Controlling pattern

## 1 Introduction

Blown sand is one of the main factors influencing road construction and operation security (Shao and Lin 2009; Mujabar and Chandrasekar 2013). Sand hazards have become more and more serious after the Qinghai–Tibet Railway was completed (Zhang et al. 2010a, b). In recent years, some studies have been conducted (Zhou et al. 2007; Liu et al. 2010). However, the sand hazard rules of Qinghai–Tibet Railway are still inadequately understood because of its unique environment with high elevation, cold temperature, and blown sand. The Honglianghe River section is located in the hinterland of Qinghai–Tibet Plateau and described as a cold and semiarid climate region with an average altitude of 4,600 m (Fig. 1). The average annual temperature is  $-4.7\text{ }^{\circ}\text{C}$ , the lowest monthly average temperature is  $-17.5\text{ }^{\circ}\text{C}$ , the highest monthly average temperature is  $6.6\text{ }^{\circ}\text{C}$ , the extreme maximum temperature is  $16.9\text{ }^{\circ}\text{C}$ , and the extreme minimum temperature is  $-30.4\text{ }^{\circ}\text{C}$ . The annual average relative humidity is 58.2 %, the annual average saturation vapor pressure is 316.9 kPa, the annual strong wind days are 136 days, and the annual average rainfall is 266 mm. Vegetation is sparse and dominated by herbaceous plants (Xie and Qu 2013), wind–sand activities are strong (Xie et al. 2012), and damage is serious. Therefore, Honglianghe River became one of the sections with the most serious sand hazards of Qinghai–Tibet Railway (Xie et al. 2013). Due to wind–sand flow accumulate and dunes moving forward, the subgrade even the rail buried, and the railway facilities destroyed, accidents such as traffic interruption and locomotive derailment occurred by sand hazards at some sections of the railway, the sand hazards seriously affect the traffic transportation. In order to control the sand hazards, some measures for sand prevention were set up. At present, three sand-blocking belts were arranged on the outer fringe of west side at Honglianghe River section of Qinghai–Tibet Railway, the total width is 150 m. Sand-blocking barrier of high vertical concrete and sand-blocking barrier of polythene net were adopted. Sand-fixing belts were arranged in the inner fringes of west side, the width is 100 m. Half-concealed checkerboard sand barriers (mainly is rocky grid) were adopted. At the east side of the railway, the settings of sand-controlling system are very similar to the west side, but the width of sand-blocking belts and sand-fixing belts is 100, 50 m, respectively. However, the effect of these measures is not ideal. Most sections were buried by sandy sediments, thus losing their sand prevention function (Fig. 2a), and artificially, cleaning sands were often needed (Fig. 2b). The Qinghai–Tibet Railway was completed and opened to traffic only in recent years, and no enough time has been allocated to further study the formation mechanism of sand hazards in Honglianghe River section. How are the sand hazards at Honglianghe River section of Qinghai–Tibet Railway formed? How to control these hazards? To answer these questions, the source of sandy materials, blown sand power environment, and the railway engineering to disturb windblown sand activity of Honglianghe River section were investigated by using methods such as field observation and analysis and indoor calculation. In addition, some prevention measures were proposed to deepen our understanding of the sand hazard rules of Qinghai–Tibet Railway and provide the basis for sand hazard prevention.

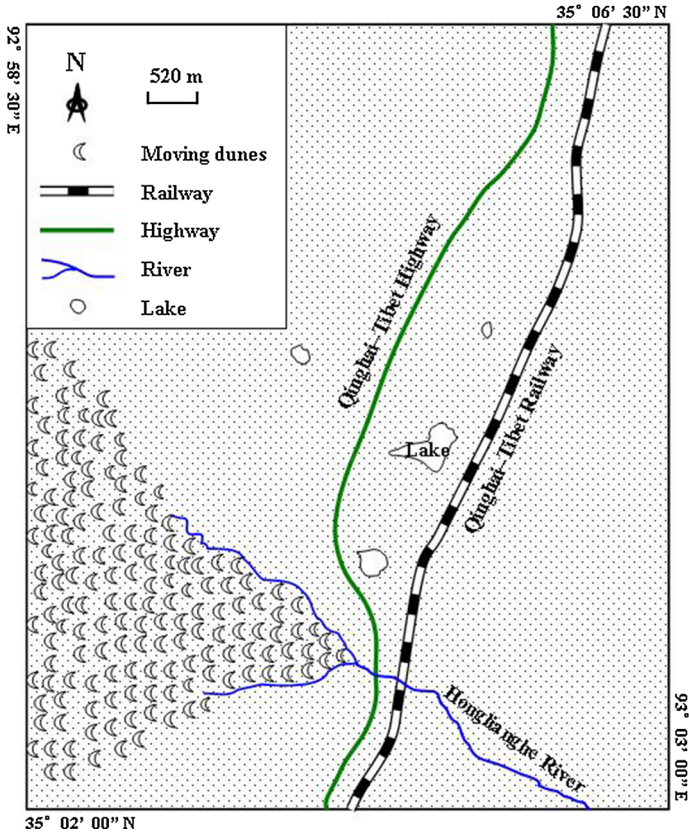


**Fig. 1** Geographical location map of Honglianghe River section of Qinghai–Tibet Railway

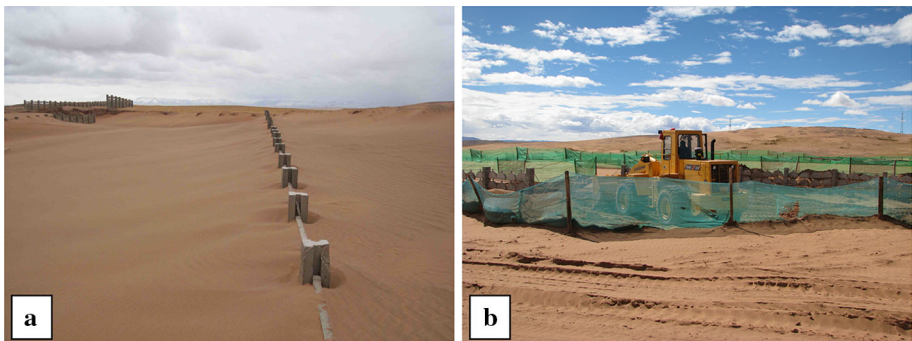


**Fig. 2** Sand hazards at Honglianghe River section of Qinghai–Tibet Railway. **a** Sand-blocking fence was buried by sandy sediments; **b** artificially clean sands

## 2 Data sources and research methods

Research data originated from observations at the Honglianghe River section of Qinghai–Tibet Railway during the year 2012 using meteorological sensors (034B wind speed and

direction sensor and HMP45C temperature and humidity sensor) at a surface height of 2 m, with wind speed and wind direction recorded every 10 min and temperature, humidity, and vapor pressure recorded every 1 h. A field wind-tunnel experiment was conducted to determine sand-moving wind in Honglianghe River section of Qinghai–Tibet Railway (Han et al. 2014). A portable wind tunnel is transported to field and installed on the surface of sand at Honglianghe River; the wind speed is increased slowly, and at the same time, the movement of sand particles at the initial stage is monitored by a high-speed camera. The critical starting speed of sand particles at Honglianghe River is found to be  $5.7 \text{ m s}^{-1}$ ; therefore, sand-moving wind in Honglianghe River section has a speed of  $5.7 \text{ m s}^{-1}$  (measured at the surface height of 2 m). Statistically, the frequencies of wind speed are greater than the sand-moving wind speed in each month based on 16 directions. Sand collected from eight directions was used to determine the sand transport rate. The vertical sand collector was used, and there are eight intakes for sand collecting corresponding to the eight directions, i.e., N ( $0^\circ$ ), NE ( $45^\circ$ ), E ( $90^\circ$ ), SE ( $135^\circ$ ), S ( $180^\circ$ ), SW ( $225^\circ$ ), W ( $270^\circ$ ), NW ( $315^\circ$ ), respectively. The section of intake for sand collecting (the height multiplied by the width) is  $1 \times 0.02 \text{ m}^2$ , a cloth bag was connected with the lower part of each intake for sand collecting, the sand blowing into the intake fall into the cloth bag, and weighing the sand in the bags regularly. The eight cloth bags placed in a round steel bucket, which buried in the ground, and the sand collector and the round steel bucket are connected by screws (Fig. 3).

Sand drift potential (DP) is calculated using the following transport equation (Lettau 1977; Bagnold 2005):

$$DP = V^2(V - V_t)t,$$

where DP is the sand DP expressed in vector units (VU). Wind speed,  $V$ , is greater than the value of sand-moving wind.  $V_t$  is the sand-moving wind speed at  $5.7 \text{ m s}^{-1}$ . The units of wind speed should be converted to  $\text{nmile h}^{-1}$ .  $t$  is the time affected by sand-moving wind and expressed in frequency, which is commonly a percentage of sand-moving wind time to total observation time in the observation period. Considering that wind is a vector, resultant drift potential (RDP) and resultant drift direction (RDD) were obtained by synthesizing the sand DP in 16 directions based on the rule of vector synthesis, which can reflect the size of the net sand transport capacity in a region. An index of the directional variability of wind is the ratio of the RDP to the DP, herein known as RDP/DP, which is used to reflect the combined situation of the wind direction in a region. Wind energy environments were classified as high energy ( $\geq 400 \text{ VU}$ ), intermediate energy ( $200\text{--}400 \text{ VU}$ ), and low energy ( $\leq 200 \text{ VU}$ ). The index of directional variability was classified as high ratio ( $\geq 0.8$ ), intermediate ratio ( $0.3\text{--}0.8$ ), and low ratio ( $\leq 0.3$ ) based on the magnitude of sand DP (Mckee 1979).

### 3 Disaster-causing mechanism of sand hazards

#### 3.1 Source of sandy material

The sand hazard sections at Honglianghe River of Qinghai–Tibet Railway have an extent of 9.76 km (K1100 + 400 to K1110 + 160) and located within  $35^\circ 02' 16''$  to  $35^\circ 06' 22'' \text{N}$  and  $93^\circ 00' 47''$  to  $93^\circ 02' 37'' \text{E}$ , with elevation ranging from 4,600 m to 4,800 m. The main landforms are the wide valley of Honglianghe River and the Gongmaorima Hill, which is a branch of Kekexili Mountain. The source of sandy material at Honglianghe River section can be traced back to Cuorendejia Lake located upriver of Qumar, where alluvial and

**Fig. 3** Sand collector at Honglianghe River section of Qinghai–Tibet Railway



diluvial materials are abundant on the lakeshore. From the Cuorendejia Lake, along the Duoergaize–Gongmaorima Mountain, to the west side of Honglianghe River section of Qinghai–Tibet Railway, a belt with a 48-km stretch of mobile sand dunes exists (Yao and Qu 2012). The section of mobile dune belt nearest the railway (straight-line distance is 790 m), with a height of 5–7 m, shows a 330° NW direction. The sand hazards of Honglianghe River section mainly come from this part of mobile sand dunes (Fig. 4a). The grain size composition of sand with particle size in the range of 0.10–0.25 mm is given priority. Sand with particle size in the range of 0.25–0.50 mm takes the second place. Sands with particle sizes in the range of 0.50–1.00 and 0.05–0.10 mm are few (Table 1) and characterized as typical eolian sand. Few sands come from alluvial and diluvial materials in the valley of Honglianghe River (Fig. 4b). The grain size composition of sand with particle size in the range of 0.10–0.25 mm is given priority, with more than 50 % of contents and other grain accounting for nearly half of the particle size of sand (Table 1).

Based on the granularity analysis of samples from far to near (from west to east) to the west side of the railway, the specific location of sand sampling as shown in Fig. 5, the result shows that sand with a particle size of 0.25–0.50 mm decreased and sand with a particle size of 0.10–0.25 mm increased gradually after the sand has traveled a certain distance. In the railway subgrade, sand with a particle size of 0.10–0.25 mm takes predominance, with contents reaching 90.6 % (Table 1). Therefore, the source of sandy



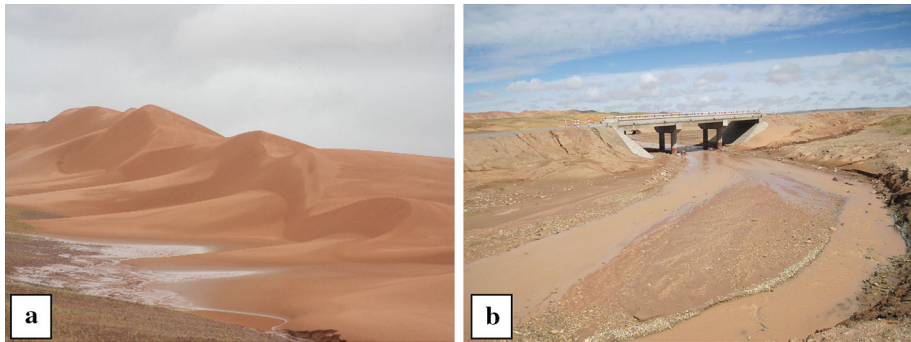


**Fig. 4** Source of sandy materials at Honglianghe River section of Qinghai–Tibet Railway. **a** Moving dune on the west side of the railway; **b** alluvial and diluvial materials in the valley of Honglianghe River

materials in Honglianghe River section is mainly transported from the west side of the railway. In the winter and spring seasons, dry particulate materials transported to the railway under the action of strong wind block and accumulate on the surface of the railway subgrade, endangering the railway.

### 3.2 Dynamic environment of wind

#### 3.2.1 Average wind velocity

During the year 2012, the average wind velocity at Honglianghe River section of Qinghai–Tibet Railway was  $3.77 \text{ m s}^{-1}$  and the maximum wind velocity was  $16.20 \text{ m s}^{-1}$ . The average wind velocity was high during the months of February, March, April, and December with 4.91, 4.13, 4.02, and  $4.22 \text{ m s}^{-1}$ , respectively. The average wind velocity was low during June to October, wherein the average wind velocity was minimum during the month of September at only  $2.93 \text{ m s}^{-1}$ . The average wind velocities during the months of January, May, and November are between these values (Fig. 6). We observed from the wind rose during the year 2012, and the N and NNW wind directions are given priority, followed by the SW wind direction. The frequency of other wind directions and static wind are low (Fig. 7).

#### 3.2.2 Conditions of sand-moving wind

The frequency of sand-moving wind is commonly a percentage of sand-moving wind time to total observation time in the observation period. The frequency of sand-moving wind during the year 2012 was 20.45 %. The frequency of sand-moving wind was high during November to May, wherein the frequency of sand-moving wind was highest during the month of February at 36.21 %. The frequency of sand-moving wind was low during June to October, wherein the frequency of sand-moving wind was lowest during the month of September at only 8.80 % (Fig. 6). The variations of sand-moving wind frequency and average wind velocity have good consistencies during the year 2012 (Fig. 6).

From the monthly dynamic rose diagram of sand-moving wind in the year 2012, sand-moving wind in Honglianghe River section followed a single direction (Fig. 8). In particular, July and September is given priority, with wind directions of NNE and W,

**Table 1** Granularity composition of sandy materials at Honglianghe River section of Qinghai–Tibet Railway (the sampling sequence from west to east)

No.	Granularity (%)							
	0.005–0.05 mm	0.05–0.10 mm	0.10–0.25 mm	0.25–0.50 mm	0.50–1.00 mm	1.00–2.00 mm	>2 mm	
1	0	0.24	60.03	36.33	3.4	0	0	0
2	0	0.9	66.93	31.46	0.7	0	0	0
3	0	0.7	73.97	25.5	0.1	0	0	0
4	0	0.54	78.03	21.13	0.3	0	0	0
5	0	1.17	87.04	11.73	0.07	0	0	0
6	0	0.94	89.03	9.93	0.1	0	0	0
7	0	1.14	89.07	9.8	0	0	0	0
8	0	7.36	90.6	2.04	0	0	0	0
9	5.33	8.73	51.6	15.53	3.43	3.03	12.34	

1 high mega dune on the west side of the railway, 2 moving dune nearest the railway, 3 sand approximately 600 m from the railway, 4 sand approximately 450 m from the railway, 5 sand approximately 300 m from the railway, 6 sand approximately 200 m from the railway, 7 sand approximately 100 m from the railway, 8 sandy sediments on the ballast of the railway, 9 valley of Honglianghe River

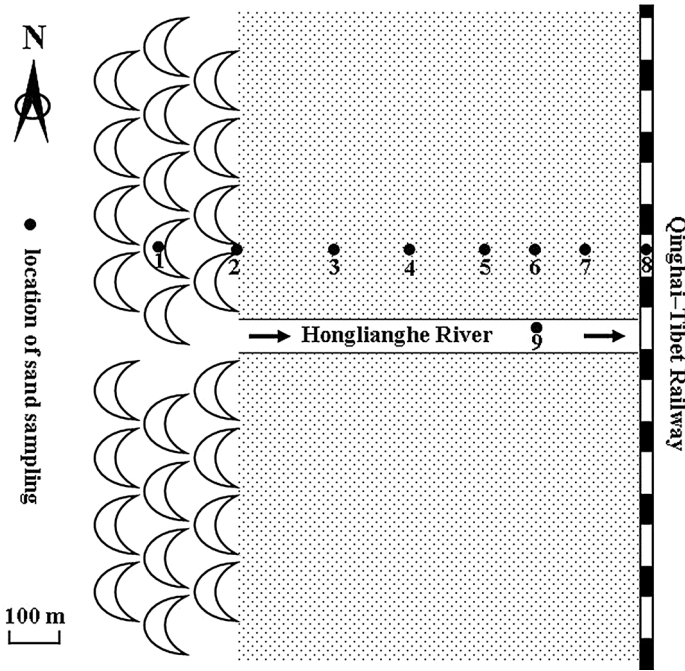
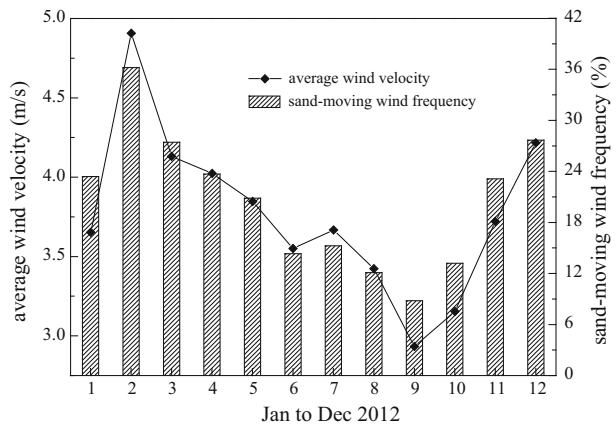


**Fig. 5** Location map of sand sampling at Honglianghe River section of Qinghai–Tibet Railway

**Fig. 6** Monthly variations of average wind velocity and sand-moving wind frequency at Honglianghe River section of Qinghai–Tibet Railway during the year 2012



respectively. The other months are mainly grouped into three wind directions of N, NNW, and NW. In particular, the N wind accounted for 78.68 and 82.19 % of the monthly total for November and December, respectively. From the dynamic rose diagram of yearly sand-moving wind, the direction of sand-moving wind is given priority, with N wind at Honglianghe River section during the year 2012 accounting for 37.45 % of the total. The NNW wind takes the second place, accounting for 25.61 % of the total. Then, the NW wind accounted for 22.10 % of the total. The frequencies of these three wind groups



**Fig. 7** Wind direction rose diagram at Honglianghe River section of Qinghai–Tibet Railway during the year 2012



static wind frequency: 1.00%  
Jan to Dec 2012

accounted for 85.16 % of the yearly total. The frequencies of the other wind directions are low (Fig. 11).

The frequency and direction of sand-moving wind were considered and synthesized as vectors. The monthly variations at Honglianghe River section of Qinghai–Tibet Railway during the year 2012 is shown in Fig. 9. The synthetic frequency of sand-moving wind is high during November to May, wherein the frequency of sand-moving wind is highest during the month of December at 98.70 %. The synthetic frequency of sand-moving wind is low during June to October, wherein the lowest was 72.31 % during August. The synthetic direction of sand-moving wind is SSE during January to June and August, S direction during July and November to December, and ESE direction during September to October. The synthetic frequency and direction of sand-moving wind were 88.53 % and 160.01°, respectively, during the whole year of 2012.

### 3.2.3 Sand drift potential

Sand DP is an important method to calculate the intensity of wind–sand activities (Wasson and Hyde 1983a, b; Hagen and Casada 2013) and an important index to measure the evolution of wind–sand landforms in a region (Lancaster 1985; Thomas 1988; Lancaster 1989). Therefore, sand DP is usually used in the design of sand prevention measures (Livingstone and Warren 1996; Bullard 1997; Genis et al. 2013). The monthly DP, RDP, RDD, and RDP/RD at Honglianghe River section during the observation period are shown in Fig. 10. The DP and RDP reached its maximum during November to March, accounting for 77.63 and 81.76 % of the yearly total, respectively, which reached a peak in February, with DP and RDP of 70.39 and 66.04 VU, accounting for 26.02 and 26.71 % of the yearly total, respectively. DP and RDP decreased gradually during April to May, from June to October at low value, with the lowest value in September at 4.25 and 3.77 VU, respectively. The seasonal variation of RDD was significant, basically at the SSE direction from January to June, S direction in July and from November to December, SE direction during August, and ESE direction during September to October. During August and October, wind direction dispersed because of an RDP/RD <0.8. The remaining months had an RDP/RD >0.8, and this high ratio shows that wind during these months followed a single direction at Honglianghe River section.

The yearly sand DP of Honglianghe River section is 270.57 VU, indicating an intermediate wind energy environment. The yearly RDP is 247.27 VU. The yearly direction variability index (RDP/DP) is 0.91, indicating a high ratio. The yearly RDD is 162.84° (Fig. 11).

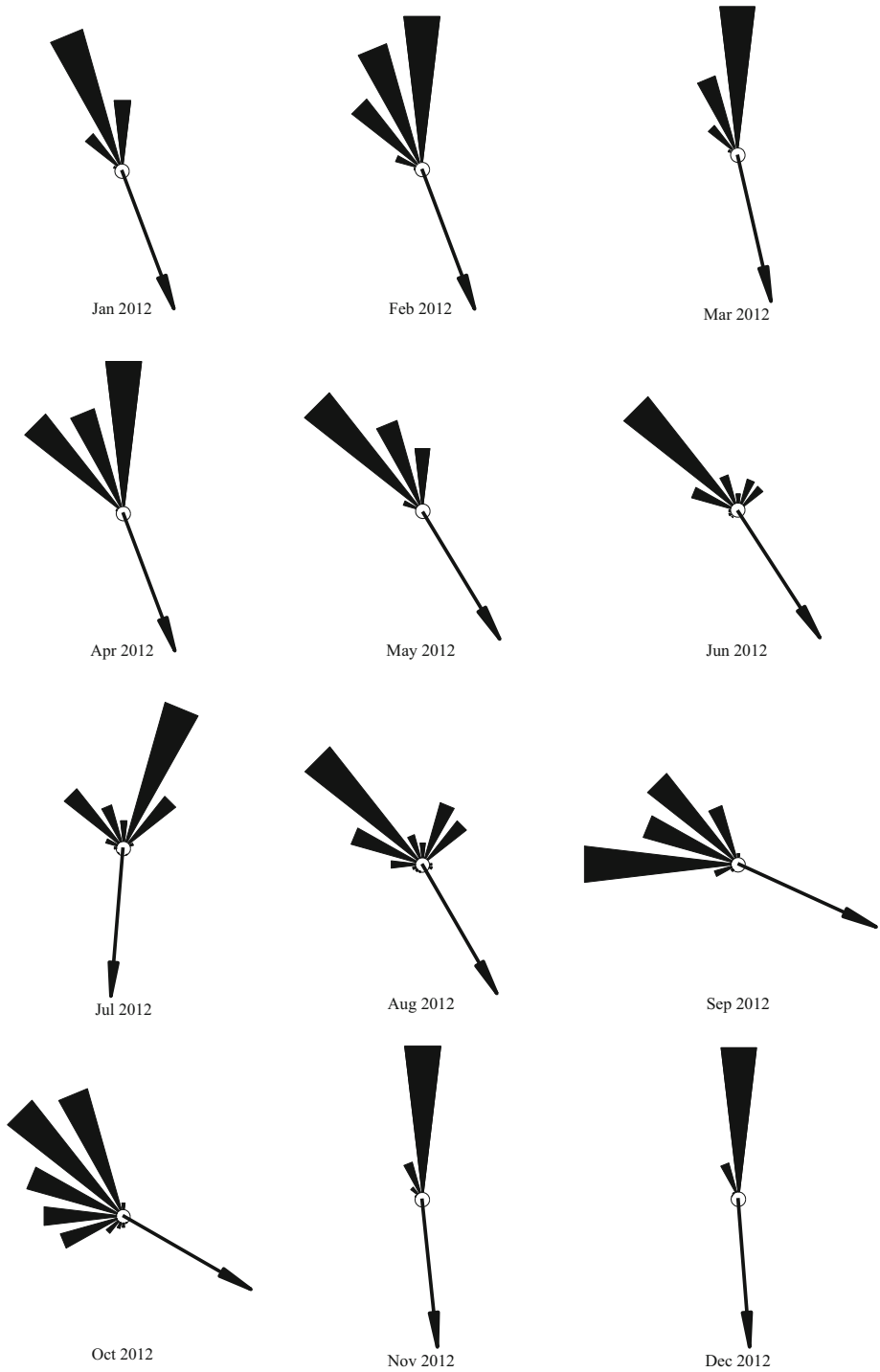
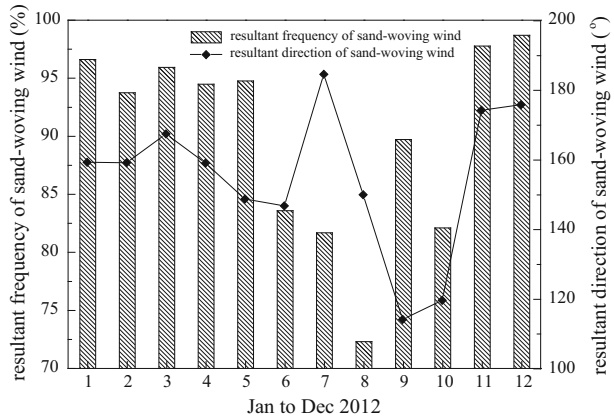


**Fig. 8** Rose of sand-moving wind at Honglianghe River section of Qinghai–Tibet Railway

**Fig. 9** Vector synthesis of sand-moving wind at Honglianghe River section of Qinghai–Tibet Railway in the year 2012



### 3.2.4 Sand transport rate

Sand transport rate was measured by using sand collected from eight wind directions at Honglianghe River section during the year 2012. The results are shown in Fig. 11. Yearly total sand transport of eight directions was  $9,959 \text{ g cm}^{-1} \text{ a}^{-1}$ , because the sand sources are located at the west side of the railway and the supply of sand materials is adequate. In addition, the three dominant wind direction groups are N, NNW, and NW (Fig. 8), with the sand transport rate of the unit width of the NW direction at its maximum, reaching  $3,925.9 \text{ g cm}^{-1} \text{ a}^{-1}$ . The N direction takes the second place, with the sand transport rate of the unit width at  $2,791.5 \text{ g cm}^{-1} \text{ a}^{-1}$ , because the N wind has the highest percentage and highest frequency of sand-moving wind (Fig. 11). The W direction has a sand transport rate of the unit width of  $1,467.3 \text{ g cm}^{-1} \text{ a}^{-1}$  because the main sand sources of the W wind is abundant. Sand transport of the three directions accounted for 82.18 % of the yearly total. The sand transport rates of the unit width of other directions are low because the sand-moving wind has a low frequency. The measured sand transport rate, the dynamic rose of sand-moving wind, and the rose of sand DP have good consistencies at Honglianghe River section (Fig. 11).

### 3.3 The railway engineering to disturb windblown sand activity

Given that the railway of Honglianghe River section tends toward the north–south direction and the valley tends toward the east–west direction approximately, the sand sources are located at the west side of the railway. The dominant wind direction tends toward the valley and across the railway. Wind–sand flow transport was blocked by the emergence of the subgrade. Based on the wind tunnel experiment of field structure of wind–sand flow above the railway subgrade along the sand hazards section of the Qinghai–Tibet Railway, it is considered that the section of railway subgrade will obviously change the flow structure of wind–sand field near ground surface, and there are the obvious blocked–rising area, collected–accelerating area, decreased–depositing area, and diffused–restoring area of airflow in a wind–sand field (Zhang et al. 2010a, b). Wind erosion occurs at the railway shoulder or the mid-upper part of railway subgrade because wind–sand flow at windward slope is forced to lift and accelerate; sand particles in the bottom layer deposit at the toe of windward section and bury the railway subgrade as wind–sand flow is enforced to lift;

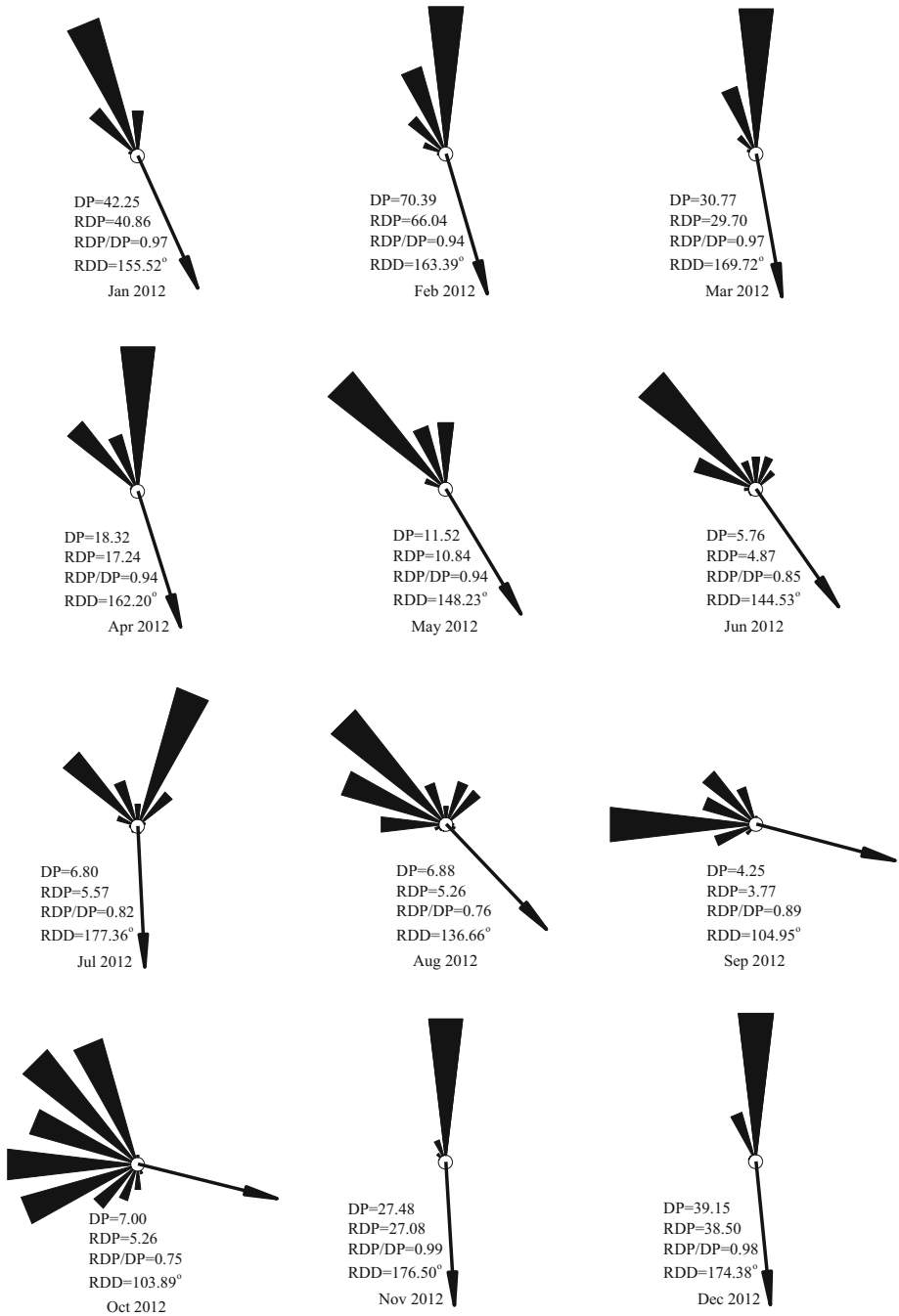


**Fig. 10** Rose of sand DP at Honglianghe River section of Qinghai–Tibet Railway

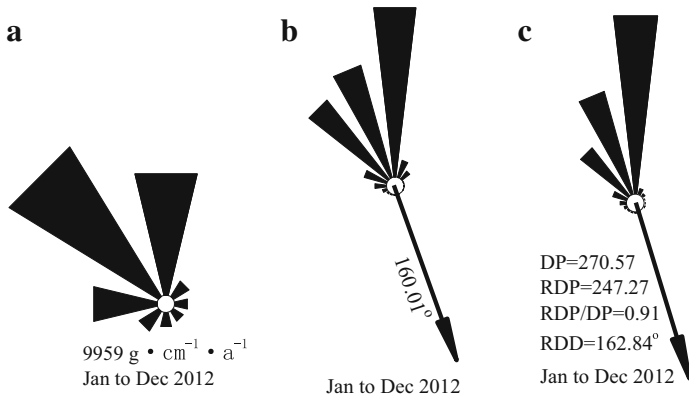


**Fig. 11** Sand transport rate of the unit width, synchronous rose of sand-moving wind, and rose of sand DP at Honglianghe River section of Qinghai–Tibet Railway. **a** Sand transport rates of the unit width, **b** rose of sand drift potential, **c** rose of sand-moving wind

wind–sand flow is in a supersaturation state and accumulates at leeward slope of the railway subgrade because of the wind speed decrease and eddy motion when airflow gets across the railway subgrade, thus causing sand materials to accumulate near the railway. Owing to the sand sources are mainly from the west side of the railway, as such, the sand sediments on the west side of the railway are especially serious hazards. The average thickness of the sand sediments on the footslope of the subgrade at the west side of Honglianghe River section was increased by 8.9 cm based on the monitoring data of intercalation signs.

#### 4 Suitable controlling pattern

The Honglianghe River section of Qinghai–Tibet Railway was characterized by the sand hazards of the valley, based on the previously presented analysis and research. Sand blocking and sand fixing were proposed as the main measures to controlling the sand hazards. Sand blocking in the outer fringe and sand fixing in the inner fringe are supplemented by sand transport and sand diversion, combined with vegetation (Fig. 12). The specific settings are as follows: Sand-blocking belts were arranged on the outer fringe of both sides of the railway. Sand-blocking barrier of high vertical concrete (with different ventilation coefficients) and sand-blocking barrier of polythene net (with different porosities) were adopted. Sand-blocking and sand-fixing barriers made of a large checkerboard of polythene net were arranged on large areas of moving dunes. Sand-fixing belts were arranged in the inner fringes. Half-concealed checkerboard sand barriers (with different sizes of rocky grid, polythene net grid, and asbestos tile grid) were adopted in the prophase stage. Grasses were cultivated to fix sands in the anaphase stage, the effect of sand fixing getting better as plants growing. The belts combining blocking and fixing were arranged on the region between the outer and inner fringes. Engineering measures such as high vertical sand barriers and water diversion controlling sand were adopted to block sands in the prophase stage. Grasses were cultivated to fix sands in the anaphase stage, grasses cultivation served by these mechanical measures just in the prophase stage. Longitudinal sand diversion walls were set up on both sides of the riverbed of Honglianghe River on a large

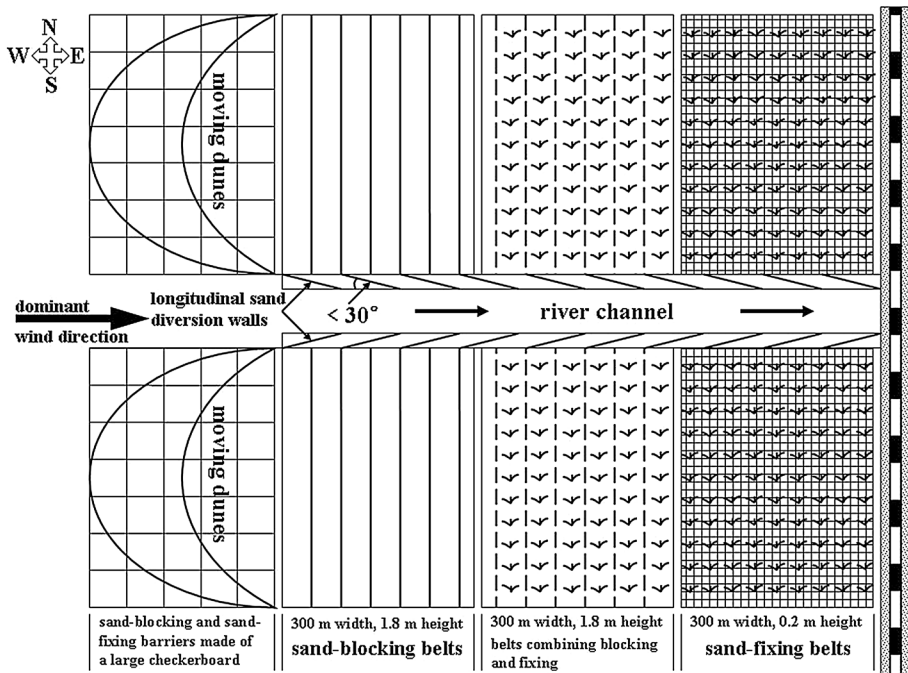


**Fig. 12** Controlling pattern of sand hazards at Honglianghe River section of Qinghai–Tibet Railway

scale. The angle to the direction of sand transport is not  $>30^\circ$ , introducing the sand into the river channel and transporting the sand away from the railway by floodwater during the flood season. Gravel packaging slopes and widening measures were adopted to protect the railway embankment. At the same time, grasses were locally grown and nurtured to strengthen artificial ecological restoration and to prevent sand hazards.

The difference between the sand-controlling pattern of authors proposed and the present sand-controlling pattern is mainly manifested in the following aspects:

The present sand-controlling pattern only the measures of sand blocking and sand fixing, and the proposed sand-controlling pattern is a comprehensive controlling system integrates sand blocking, sand fixing, sand transport, and sand diversion.

In order to suppress the sand moving, in the proposed sand-controlling pattern, sand-blocking and sand-fixing barriers made of a large checkerboard net were arranged on large areas of moving dunes at the west side of railway.

In the proposed sand-controlling pattern, a new idea which longitudinal sand diversion walls were set up on both sides of the riverbed of Honglianghe River, introducing the sand into the river channel and transporting the sand by floodwater during the flood season was suggested.

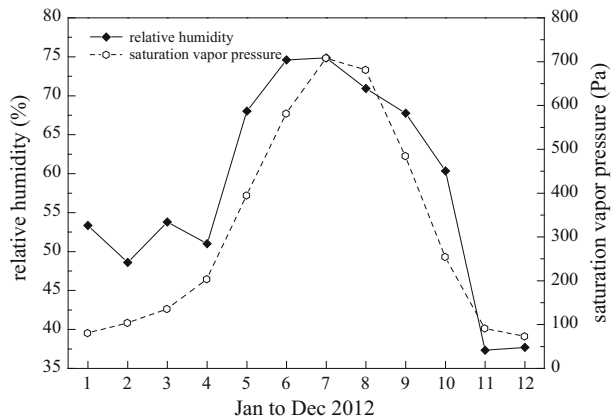
At present, the mechanical control measures are the main method used for protecting the Qinghai–Tibet Railway from sand hazards, although the protection effect is obvious in the initial stages; however, it will be buried by sand sediments and failure eventually with the passage of time. Therefore, the sand prevention of Qinghai–Tibet Railway should be dominated by biological measures (such as vegetation restoration), vegetation restoration served by mechanical measures. In the proposed sand-controlling pattern, cultivate





**Fig. 13** Grasses in the sand barriers of rocky grid at Honglianghe River section of Qinghai–Tibet Railway (Aug 2014)

**Fig. 14** Monthly variations of air humidity and vapor pressure at Honglianghe River section of Qinghai–Tibet Railway



vegetation and strengthen artificial ecological restoration were added, especially during the year 2014, grasses was cultivated in the sand barriers of rocky grid at Honglianghe River section of Qinghai–Tibet Railway, the effect of grasses on sand prevention is good (Fig. 13); therefore, the sand fixing of plants is the essential measure for protecting the Qinghai–Tibet Railway from sand hazards in the long run.

### 5 Discussion

Monthly variations of average relative humidity and average saturation vapor pressure at Honglianghe River section also increased the sand hazards based on the synchronously measured meteorological data (Figs. 14, 10). During summer from May to October, the sand

hazards are not serious because of more precipitation, high vapor pressure, humid air, high water content of the surface sand layer, small average wind velocity, low frequency of sand-moving wind, and less strong wind days. During winter from November to April, the sand hazards are serious because of scarce precipitation, low vapor pressure, dry air, low water content of the surface sand layer, large average wind velocity, high frequency of sand-moving wind, and more strong wind days. In addition, most of the riverbeds are bare in the dry season. In particular, during the end of the cold season and at the beginning of the warm season, river sediments are loosened, broken up, or melted. Sandy materials were blown up and transported easily under the action of strong wind, encountered the barriers of the railway, and accumulated, thus causing disaster. Therefore, the sand hazards of Honglianghe River section were exacerbated further by strong winds and dry synchronous overlap in winter.

## 6 Conclusions

Through this research, the following conclusions can be made:

The sand sources of Honglianghe River section are abundant and are mainly from the sandy hill of the west side of the railway. The grain composition of sand with particle size in the range of 0.10–0.25 mm is given priority.

The yearly sand-moving wind of Honglianghe River section is mainly from the N, NNW, and NW directions. The frequencies of these three wind groups accounted for 85.16 % of the yearly total. Therefore, the sand hazards of the three directions are serious because the sand sources concentrated on the west side of the railway, with the most serious sand hazards located at the NW direction of the railway. In particular, during the colder half of the year, the average wind velocity is high, the frequency of sand-moving wind is high, and the sand hazards are most serious.

The yearly sand DP of Honglianghe River section is 270.57 VU, indicating an intermediate wind energy environment. The yearly RDP is 247.27 VU. The yearly direction variability index (RDP/DP) is 0.91, indicating a high ratio. The yearly RDD is 162.84°. In particular, during November to March, the DP and RDP reached its maximum, accounting for 77.63 and 81.76 % of the yearly total, respectively, which reached a peak in February, with DP and RDP of 70.39 and 66.04 VU, accounting for 26.02 and 26.71 % of the yearly total, respectively. The yearly RDP/RD, which is >0.9, indicates that the wind followed a single direction.

The disaster-causing mechanism of the sand hazards of Honglianghe River section is described as follows: In windy dry season (during the colder half of the year), the loose and broken sand materials are blown up by wind, forming wind–sand flow and movement, which are then disturbed by the railway subgradation and sand accumulation, thus causing disaster. Therefore, the sand hazards of Honglianghe River section mainly occur during the winter half of the year and are mostly concentrated and distributed at the west side of the railway.

The Honglianghe River section of Qinghai–Tibet Railway was characterized by the sand hazards of valley. Sand prevention measures should be dominated by sand blocking and sand fixing, namely sand blocking in the outer fringe and sand fixing in the inner fringe, supplemented by sand transport and sand diversion, combined with vegetation. Sand-blocking belts were arranged on the outer fringe of the railway, whereas sand-fixing belts were arranged on the inner fringes. Longitudinal sand diversion walls were set up on both sides of the riverbed. At the same time, grasses were local grown and nurtured to strengthen artificial ecological restoration.

**Acknowledgments** This research project funded by the National Natural Science Foundation of China (Grant No. 41401611), China Postdoctoral Science Foundation (Grant No. 2014M560817), Foundation for Excellent Youth Scholars of Cold and Arid Regions Environmental and Engineering Research Institute, Chinese Academy of Sciences (Grant No. 51Y351121), and Science and technology program of Gansu Province (Grant No. 145RJZA118). The authors would like to thank the two anonymous reviewers' useful comments and the editor's valuable suggestions for improving this manuscript.

## References

- Bagnold RA (2005) *The physics of blown sand and desert dunes*. Dover Publications Inc, Mineola, pp 57–76
- Bullard JE (1997) A note on the use of the “fryberger method” for evaluating potential sand transport by wind. *J Sediment Res* 67:499–501
- Genis A, Vulfson L, Ben-Asher J (2013) Combating wind erosion of sandy soils and crop damage in the coastal deserts: wind tunnel experiments. *Aeolian Res* 9:69–73
- Hagen LJ, Casada ME (2013) Effect of canopy leaf distribution on sand transport and abrasion energy. *Aeolian Res* 10:37–42
- Han QJ, Qu JJ, Dong ZB et al (2014) The effect of air density on sand transport structures and the adobe abrasion profile: a field wind-tunnel experiment over a wide range of altitude. *Bound-Layer Meteorol* 150(2):299–317
- Lancaster N (1985) Wind and sand movement in the Namib sand sea. *Earth Surf Proc Land* 10:607–619
- Lancaster N (1989) The dynamics of star dunes: an example from the Gran Desierto, Mexico. *Sedimentology* 36:273–289
- Lettau K, Lettau H, (1977) *Experimental and micrometeorological field studies of dune migration. Exploring the world's driest climate*. University of Wisconsin-Madison, pp 110–147
- Liu SH, Feng LZ, Xu ZY (2010) Study on effect of wind erosion controlling in the Geermu-Lhasa section of the Qinghai–Tibet Railway. *J China Railw Soc* 32(1):133–136
- Livingstone I, Warren A (1996) *Aeolian geomorphology: an introduction*. Addison Wesley Longman Limited, London, pp 22–23
- Mckee ED (1979) *A study of global sand seas*. University Press of the Pacific, Honolulu, pp 137–169
- Mujabar PS, Chandrasekar N (2013) Coastal erosion hazard and vulnerability assessment for southern coastal Tamil Nadu of India by using remote sensing and GIS. *Nat Hazards* 69(3):1295–1314
- Shao L, Lin BL (2009) Environment impact assessment of desert railway based on fuzzy comprehensive evaluation. *J China Railw Soc* 31(5):84–89
- Thomas DSG (1988) The nature and deposition setting of arid and semi-arid Kalahari sediments, southern Africa. *J Arid Environ* 14:17–26
- Wasson RJ, Hyde R (1983a) A test of granulometric control of desert dune geometry. *Earth Surf Proc Land* 8:301–312
- Wasson RJ, Hyde R (1983b) Factors determining desert dune type. *Nature* 304:337–339
- Xie SB, Qu JJ (2013) Analyses on the types, distributions distributions and characteristics of vegetation and soil along Qinghai–Tibet Railway. *Meteorolog Environ Res* 4(9):15–18
- Xie SB, Qu JJ, Zu RP et al (2012) New discoveries on the effects of desertification on the ground temperature of permafrost and its significance to the Qinghai–Tibet plateau. *Chin Sci Bull* 57(8):838–842
- Xie SB, Qu JJ, Zu RP et al (2013) Effect of sandy sediments produced by the mechanical control of sand deposition on the thermal regime of underlying permafrost along the Qinghai–Tibet Railway. *Land Degrad Dev* 24:453–462
- Yao ZY, Qu JJ (2012) Source and grain size of Aeolian aeolian sands along Golmud-Lhasa section of Qinghai–Tibet Railway. *J Desert Res* 32(2):300–307
- Zhang KC, Niu QH, Qu JJ et al (2010a) Study on the characteristics of flow field and the mechanism of wind-blown sand disasters in the Tuotuohe region along the Qinghai–Tibet Railway. *Arid Zone Res* 27(2):303–308
- Zhang KC, Qu JJ, Liao KT et al (2010b) Damage by wind-blown sand and its control along Qinghai–Tibet Railway in China. *Aeolian Res* 1:143–146
- Zhou D, Tian HQ, Yang MZ et al (2007) Comparison of aerodynamic performance of different kinds wagons running on embankment of the Qinghai–Tibet Railway under strong cross-wind. *J China Railw Soc* 29(5):32–36